SPOT WELDING PARAMETERS INFLUENCE ON THE ASSEMBLED STRUCTURES BEHAVIOR

S. Guezzen[1], M. C. Djamaa[2]*, M. Amirat[1], A. Hadjoui[1]

[1]Department of Mechanical Engineering, University Abou Bekr Belkaid, Tlemcen, Algeria
[2]Laboratory of Mechanics & Structures, University 8 May 1945 – Guelma, Guelma, Algeria
*Corresponding author's e-mail address: djamaa.mohamedcherif@univ-guelma.dz

ABSTRACT

Resistance spot welding (RSW) remains a critical joining technique in the automotive and aerospace industries due to its efficiency in assembling thin metallic sheets. However, the mechanical integrity of spot welds is often compromised by tensile stresses perpendicular to the weld plane, leading to premature failure. This study proposes a systematic experimental approach to quantify the influence of welding parameters, such as current intensity, electrode pressure, and welding time, on the tensile strength of welded joints. The novelty of this work lies in establishing a direct correlation between process parameters and joint performance to maximize weld strength without compromising microstructural integrity. Hardness tests confirmed that the hardness of the weld point depends on the initial microstructure of the base material and on the welding conditions. The results demonstrate that increasing current and welding time within controlled limits enhances nugget formation and joint resistance by up to 25% compared to conventional settings. These findings provide valuable insights for optimizing RSW processes to achieve reliable and high-quality assemblies.

KEYWORDS: resistance spot welding, steel assembly, tensile stress

1. INTRODUCTION

Resistance spot welding is one of the most widely employed joining techniques in the automotive, aerospace, and mechanical industries due to its high productivity, cost-effectiveness, and ability to achieve precise assemblies of thin metal sheets. Originally patented by J. Thomson in 1877, the process relies on the Joule effect where a high-intensity electric current passes through sheets pressed together by electrodes, producing localized heating at the interface. The resulting molten nugget solidifies under electrode pressure to form a weld joint. Despite its apparent simplicity, RSW involves a complex coupling of electrical, thermal, and mechanical phenomena that critically influence weld quality, microstructural evolution, and mechanical performance.

Extensive research has been devoted to understanding how process parameters, such as welding current, time, and electrode force affect joint performance. Chen et al. [1] investigated the shearing strength of resistance spot-welded joints between dissimilar steel plates by varying welding current and welding time. The researchers used 1mm thick steel plates with a medium-frequency spot welding machine, applying a constant force of 3.6kN through Cr-Zr-Cu electrodes. The optimal welding parameters were identified as 10kA current and 80ms welding time, achieving maximum shearing strength of 7504.67N. The study revealed two fracture modes: 'shearing-off' for lower strength joints and 'peeling' for higher strength joints, with peeling indicating superior joint quality. Microstructural analysis showed five distinct regions in the welded joints, with the nugget exhibiting the highest micro-hardness due to martensite formation. The nugget size was larger on the stainless steel side due to its lower thermal and electrical conductivity compared to low carbon steel, which increased with both welding current and time. The heat-affected zones showed that the coarse microstructure having higher hardness than fine one due to martensite presence. Shojaee et al. [2] investigated the effect of loading orientation (0° to 90°) on mechanical properties and failure modes of resistance spot welds in third-generation advanced high-strength steels. An innovative Digital Image Correlation-based testing methodology is developed to accurately measure peak load, energy absorption, and failure characteristics so ultimately finding that 3G-980 welds demonstrate superior energy absorption compared to 3G-1180. Both materials showing substantial peak load reductions (65-81%) as loading transitions from pure shear to pure tension, providing critical data for improving automotive crash safety

Date of submission/acceptance: 24.02.2025/15.12.2025
https://doi.org/10.35219/awet.2025.04

simulations. Similarly, Chen et al. [3] investigated the microstructure and mechanical properties of WC-10Co-RM80 steel dissimilar resistance spot welding joints. The study evaluates mechanical properties through shear tests and analyzes the evolution of weld pools under varying welding currents, which influence temperature distribution within different zones of the joint and its impact on deformation and the formation of weld slag. The research highlights that excessive welding current can lead to rapid heating and cooling, extrusion of weld slag, and crack formation, ultimately affecting the bonding strength of the welded joints. Anijdan et al. [4] optimized spot welding parameters for dissimilar joints of DP600 dual-phase steel and AISI 304 stainless steel, aiming to achieve maximum shear-tensile strength. Using the Taguchi method and Minitab software, the study identified current density, holding time, welding time, and electrode force as critical parameters influencing joint strength. A microstructural analysis of the welded joints shows a fully martensitic weld nugget and a microstructural gradient in the heat-affected zone of DP600 steel. High cooling rates, potentially exceeding 1000°, were noted as spot welding process characteristic for these materials.

However, while prior works have successfully characterized the effects of individual parameters, they often lack an integrated analysis of the combined mechanical and metallurgical factors governing weld behaviour, where several studies have also addressed the role of the base metal microstructure. Shirmohammadi et al. [5] specifically focused on the impact of the initial base metal microstructure on the weld's microstructure and mechanical performance of martensitic stainless steel. Authors evaluate joint behaviour through tensile-shear tests and microhardness measurements by varying the welding parameters, such as a welding current range of 7-11kA and a welding time of 0.2s. Key findings include that increasing welding current enhances the fusion zone size, which its microstructure primarily consists of martensite and some δ-ferrite due to rapid cooling rates and the presence of ferrite-promoting elements. Costa et al. [6] investigated the mechanical behaviour of hybrid joints, which combine resistance spot welding and adhesive bonding. The authors proposed experimental procedure, which aims to demonstrate that these hybrid joints exhibit superior performance, while adhesive bonding process itself appears to be sensitive to temperature extremes.

The hybrid joining techniques are applied in aerospace and automotive due to their potential for increased static strength, fatigue strength, energy absorption, and corrosion resistance. Eshraghi et al. [7] proposed a thermomechanically-coupled finite element analysis to highlight the effects of resistance spot welding parameters on weld pool properties in DP600 dual-phase steel. The study employs different techniques to analyse responses such as nugget radius, nugget thickness, heat-affected zone radius, and molten zone volume following various spot welding parameters and their interactions. The findings indicate that only the interaction between current intensity and electrode face radius significantly impacts nugget radius, nugget thickness, and molten zone volume. Florea et al. [8] conducted an experimental study on the influence of spot welding parameters on the fatigue life and microstructure of the weld spot of a 6061-T6 aluminum alloy. Researchers conducted cyclic fatigue tests on 36 coupons under various load ratios and welding conditions, where complete failure is observed at a frequency of 10Hz. The study also utilized Scanning Electron Microscopy for post-fatigue microstructure analysis and fractography, focusing on interfacial failure modes at nominal conditions. The main goal was to correlate process parameters with weld quality and understand their impact on fatigue performance. In a recent study, Lin and Chang [9] propose a monitoring system for micro-series resistance spot welding using dual accelerometers, mounted above each electrode holder. The developed signal was successfully captured and twice integrated to reflect an expansion/contraction of the electrode motion in order to analyse the thermophysical phenomena during the RSW process. Wang and Zhang [10] investigated the effects of different welding parameters and types of nuts on resistance projection welding of nuts to sheets. The analysed microstructures show that the welded joint size and the failure mode of welded joints were performed in which the microhardness distribution of the fusion zone gradually becomes homogeneous with the increase of the welding current or the welding time. Han et al. [11] proposed a study to optimize the shape of square nut for better projection welding performance where the difference of set down values between experiments and FEA is within 12%, which verify the reliability of the FE model.

Therefore, the present study aims to investigate systematically the combined influence of sheet thickness, mechanical properties of the base material, and key RSW parameters like current, time, and electrode pressure on the mechanical behaviour of spot-welded assemblies. Special attention is given to tensile loading perpendicular to the weld plane, a critical condition that often governs service life. Through a series of controlled experiments and mechanical tests, this work seeks to establish quantitative relationships between welding parameters and joint performance.

2. SPOT WELDING PRINCIPLE

Resistance spot welding, figure 1, is a localized fusion joining process in which a high-density electric current, combined with electrode pressure, induces resistive heating at the interface of overlapping sheets. As a result, a transient molten nugget is produced and solidified under constraint, yielding a joint composed of a fusion zone, heat-affected zone, and unaffected

zone, whose microstructural evolution and mechanical performance are governed by the complex interaction between different welding condition.

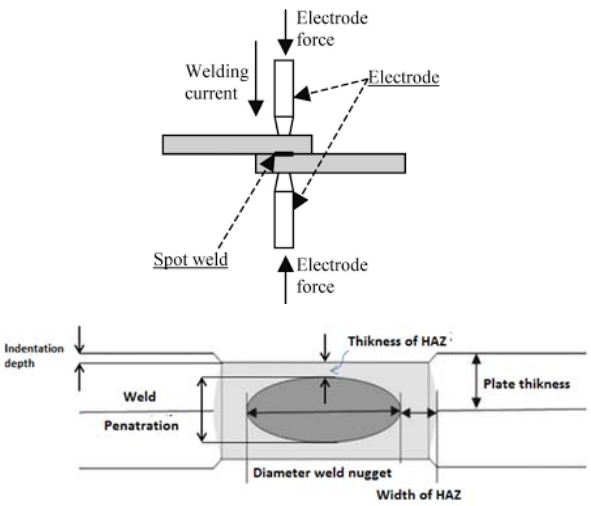

Fig. 1. Illustration of resistance spot welding process

This process implements the Joule effect of a high intensity current. The heat produced is expressed by the following formula:

$$Q = \int_0^T RI^2 dt \quad (1)$$

where R is the total electrical resistance, I the current traveling between electrodes and t is the time.

The formulation assumes that the total electrical resistance at the weld nugget remains constant during the passage of current. However, in practice, this resistance slightly decreases as the temperature increases. Thermal losses arise from several heat dissipation paths through which the heat generated at the weld nugget escapes, including through the electrodes, through the surrounding sheets near the weld zone and a small fraction of the generated heat is lost by radiation to the ambient air. The main factors influencing the resistance at the interface between sheets include the surface roughness, electrode clamping pressure, electrode material and geometry.

To account for the thermal losses occurring during resistance spot welding, an efficiency coefficient η is introduced:

$$Q_e = \eta RI^2 t \quad (2)$$

where Q_e represents the effective heat used to melt the metal and form the weld nugget.

This formulation allows for proper adjustment of the welding current and time to achieve a sound joint quality. The η coefficient depends on several parameters, including the material type (from 0.75 to 0.9 for mild steels, 0.6 to 0.8 for galvanized steels, and 0.5 to 0.7 for stainless steels), sheet thickness, electrode hardness, and welding duration. Neglecting this coefficient leads to an overestimation of the amount of metal melted during welding.

3. MATERIALS AND METHODS

3.1. Materials

The welding process was carried out on the spot welding machine AROMA 350 DC (Fig. 2). The machine has a power of 30kVA at 50%, a performance of 21kVA at 100% and a maximum welding capacity of 156kVA.

The applied pressure, directly displayed in bar, is obtained by the machine's pneumatic system and controlled using an air pressure regulator and the corresponding force between electrodes can ~~reached~~ reach 730daN.

The machine's electrodes are made of a copper-chromium-zirconium (CuCrZr) alloy, a material that offers excellent electrical and thermal conductivity as well as good mechanical wear resistance. Their truncated cone shape with a flat contact face is well-suited to the thickness of the sheets being welded. The total length of the electrodes is 100mm, providing good rigidity and efficient cooling and the cone angle of 120° guaranteed uniform current distribution to the contact area.

The general criterion for spot welding, which defines the electrode diameter (D) as a function of the sheet thickness (E), is given by the following formula:

$$D = 5\sqrt{E} \quad (3)$$

In this study, for 2mm thicknesses, a diameter of 7mm is used, while for thinner sheets, a diameter of 6mm is employed.

Fig. 2. Spot welding equipment

The first step involves cutting the samples from a sheet of metal using a punch press to give them the same shape. Burrs and sharp edges must be removed to guarantee uniform contact between the samples to be welded.

The next step involves initial degreasing with acetone to remove the oil layer from the surfaces, light sanding of the weld overlap area, air blowing, and then general cleaning with alcohol. Before starting the welding operation, the flatness of the samples was checked so that the sheets were pressed together without any gaps. In order to prevent the sheets from slipping during the closing of the electrodes, a positioning and clamping clamp is used.

The steel sheets having a thickness of 2mm were cut to the dimensions of 100mm by 20mm where each two sheets are welded at a single point on the middle-overlapped area of 25mm by 20mm (Fig. 3).

In order to determine the influence of thickness, mechanical properties and welding parameters on the mechanical behaviour of spot-welded structures, experimental tests on several samples of welded sheets are performed on a computer-controlled universal tensile machine with an estimated tensile capacity of 600KN. To study the influence of the type of sheets materials, three types of steel are used: mild steel, galvanized steel and stainless steel. Chemical composition, physical and mechanical properties of the used materials are listed in tables 1-3 [13-15].

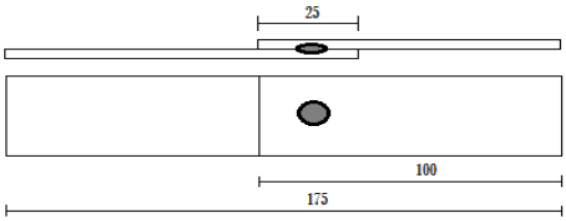

Fig. 3. Welded sheet specimen

Table 1. Chemical composition

Type of steel	Fe	C	Mn	P	S	Si	Cr	Ni
Mild Steel (DC03)	98%	≤0.10%	≤0.45%	≤0.035%	≤0.035%	≤0.04%		
Stainless steel (304L)	78%	≤0.030%	≤2%	≤0.045%	≤0.030%	≤1%	17.5-19.5%	8-10%
Galvanized steel (Z275)	86%	<0.18%	<1.2%	<0.12%	<0.045%	<0.50%		

Table 2. Physical properties

Type of steel	Density [Kgm^{-3}]	Electrical resistivity [$\mu\Omega cm^{-1}$]	Specific heat [$Jkg^{-1}K^{-1}$]	Thermal conductivity [$Wm^{-1}K^{-1}$]	Linear expansion coefficient
Mild Steel (DC03)	7800	11	450	46	12
Stainless steel (304L)	8000	72	500	16.2	18
Galvanized steel (Z275)	7100	5.9	380	0.035	23.5

Table 3. Mechanical properties

Type of steel	Elasticity limit, Re [MPa]	Breaking strength, Rm [MPa]	Elongation, A [%]
Mild Steel (DC03)	240	270-350	34
Stainless steel (304L)	200-220	500-670	45
Galvanized steel (Z275)	---	270-500	22

3.2. Methods

The weld assemblies are mounted between two tensile clamps and the load is applied at constant speed. We present different results of the tensile tests carried out on several samples of welded sheets assembled at different conditions by varying the type of materials, thicknesses, current intensity, welding time, the applied force between electrodes. The aim of the tensile tests is to determine the maximum force applied until the break of the weld point as well as the tensile curves, which show the dependence between the applied force and the elongation. The collected data are used to analyse the mechanical behaviour of the different samples until break.

Hardness tests are performed to estimate the hardness of specimens on the unaffected zone of the base material and others tests exactly on the weld points of assembled sheets according to different key process parameters as the material type, the welding cycles, the applied pressure, the current intensity, and sheet thickness using AFFRI METALTEST MIKII portable hardness tester. This static indentation device is capable of testing a wide range of materials for thin sheets and provides a direct Vickers hardness reading.

The averaging hardness, measured on the unaffected zone on all specimens, are given as follows:

the hardness of stainless steel 304L is 185HV, the one of galvanized steel Z275 is 120HV and of 115HV for mild steel DC03.

4. RESULTS AND DISCUSSION

4.1. Material Grade

In order to determine the influence of the material on the hardness of the weld point and the strength of the welded sheets, three specimens made with mild steel, galvanized steel and stainless steel are tested at the following conditions (Table 4).

Table 4. Experimental welding conditions of the tensile test N°1

Tested specimens	**P1**	**P2**	**P3**
Variable parameter: Material type	Mild Steel (DC03)	Stainless steel (304L)	Galvanized steel (Z275)
Input parameters	T=18 cycles, I=14 KA, e=2 mm and P=6 bars		

Under these welding conditions, the estimated hardness values on the welding point show that stainless steel 304L presents the highest hardness of 190HV, which is close to that of the base metal. The hardness of galvanized steel Z275 is higher than of mild steel DC03 (Fig. 4). In the case of the stainless steel, the negligible variation between the hardness of the base metal and that of the weld point is due to the base microstructure, which is composed primarily of martensite like the fusion zone, whose microstructure consists of martensite and some δ-ferrite. However, for the two others materials, the hardness upgraded about 20% compared to the base metal. The weld point undergoes very rapid thermal cycles (heating then cooling), which can lead to a hardening phenomenon according to the formation of harder microstructures.

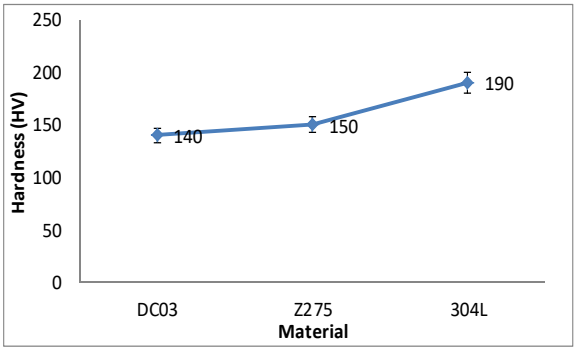

Fig. 4. Effect of material type

The specimens subjected to tensile testing are exhibited in figure 5.

Fig. 5. Broken specimens after the tensile test for different materials: P1 at the top, P2 in the middle and P3 at the bottom

The corresponding evolution curve relating the load to the displacement up to failure of the spot welded sheets are shown in figure 6.

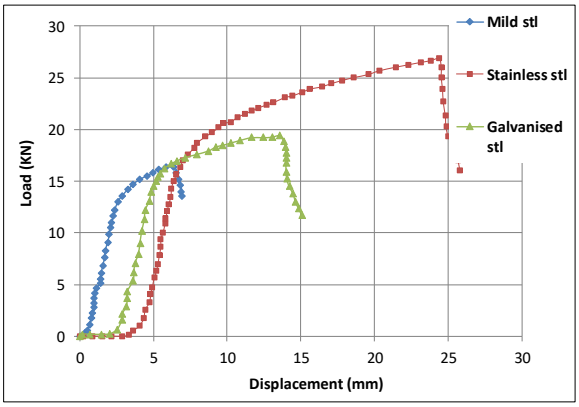

Fig. 6. Effect of the material type on the mechanical behaviour of the welded sheets according to the test protocol N°1

From figure 6, the curves shape resembles to an ordinary tensile test. It can be seen that the collapse of welded assemblies is differentiated according to the mechanical characteristics of each material.

In the case of mild steel, the welded zone has a hardness higher than of the base material and therefore the elongation of welded assembly depends on the behavior of base material, which quickly collapses as soon as the load reaches approximately 17KN at an equivalent displacement of 7mm.

For the case of galvanized steel, it behaves like the first one since the displacement reached is approximately 14mm for a load of 19KN.

For the stainless steel assembly, its mechanical behaviour is even better with a clearly visible collapse resistance, characterized by an approximate displacement of 24mm following a load reaching 27KN. The weld point characteristics are practically the same of the base material (same hardness) and therefore the welded assembly behaves as a single component.

The precise values of the maximum load Fm, the load at the lower yield limit Fe_L, the load at the upper yield limit Fe_H, the lower yield strength Re_L, the upper yield strength Re_H and tensile strength Rm are given in table 5. From these results, we can say that the resistance of the welding point in the case of stainless steel sheet is the greater because the mild steel may contain impurities or a corrosive layer, which can weaken the strength of the welding point comparing to the stainless steel.

Table 5. Variation of loads and stresses according to the material type of the welded sheets

Results	P1 Mild steel	P2 Stainless steel	P3 Galvanized steel
Fm [kN]	16.382	26.887	19.431
Fe_L [kN]	16.382	22.773	18.99
Fe_H [kN]	16.382	22.883	19.1
Rm [MPa]	409.55	672.177	485.767
Re_L [MPa]	409.55	569.33	474.748
Re_H [MPa]	409.55	572.085	477.502

In order to show the influence of the base material on the weld point dimensions, the welding of six tested samples was carried out. Two mild steel, two galvanized steel and two stainless steel under the same conditions as the test N°1. After the welding process, the welded point diameters were measured as mentioned in table 6.

Table 6. Weld point dimensions for different welded materials

Spot dimensions		P1 Mild steel	P2 Stainless steel	P3 Galva. steel
Welding point dimensions [mm]	Test 1-1	12.2	10.3	8.2
	Test 1-2	12.2	10.2	8.1

It can be observed that the diameter of the welding point in the case of mild steel is larger than that of stainless steel or galvanized steel. This is due to the difference in the thermal properties of the materials, mainly the thermal conductivity and the coefficient of thermal expansion, which is higher for mild steel than for other materials. In fact, the surface layer of zinc of galvanized steel helps to reduce thermal effects and prevents the heat transfer to the middle layer of the plates, which gives rise to a spot weld of smaller dimensions. The same observation is valid for stainless steel, which unlike mild steel and galvanized steel, contains less carbon and a high percentage of chromium and nickel, which influence negatively the thermal conductivity of this material.

4.2. Welding Time

In order to determine the influence of the time on the hardness of the weld point and the strength of the welded sheets, three specimens made with mild steel are tested at the conditions presented in table 8. The welding time was varied between 16, 18, and 25 cycles while keeping other parameters constant.

Table 7. Experimental welding conditions of the tensile test N°2

Tested specimens	P4	P5	P6
Variable parameter: Welding time (Cycle)	T=16	T=18	T=25
Input parameters	Mild Steel (DC03), I=14 KA, e=2 mm, P=6 bars		

A gradual decrease in hardness is observed with increasing number of welding cycles (Fig. 7). This trend indicates that prolonged thermal exposure promotes local softening, likely due to grain growth within the heat-affected zone.

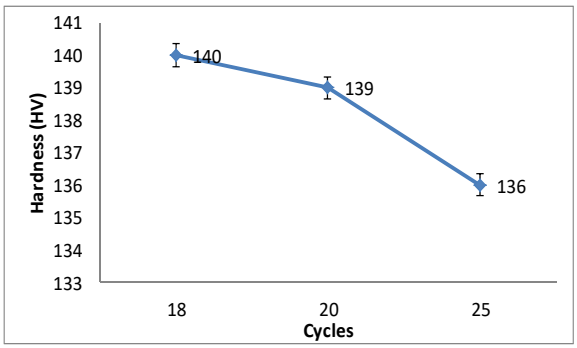

Fig. 7. Effect of welding cycles

The specimens after the tensile tests are photographed as shown in figure 8 and the evolution curve relating the load to the displacement until the failure of the spot welded sheets is shown in figure 9.

Fig. 8. Broken specimens after the tensile test for different welding times: P4 at the top, P5 in the middle and P6 at the bottom

It can be seen that increasing the welding time leads to an increase in the maximum load, more significant in the range from 16 cycles to 18 cycles but a less for 25 cycles.

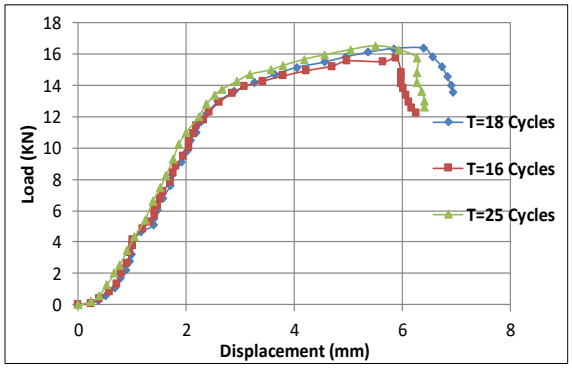

Fig. 9. Effect of welding time on the mechanical behaviour of the welded sheets according to N°2 test

From figure 9, one can obtain the results concerning the loads and stresses as a function of the welding time (Table 8).

Table 8. Variation of loads and stresses according to the welding time

Results	T= 16 cycles	T= 18 cycles	T= 25 cycles
Fm [kN]	15.758	16.382	16.529
Rm [MPa]	393.94	409.55	413.223

As shown in figure 9 and table 9, increasing the welding time from 16 to 18 cycles improved the tensile strength significantly (Rm rose by ~4%). However, extending it to 25 cycles resulted in only a marginal improvement (~0.9%), indicating a saturation threshold. Beyond this point, further heat input offers little mechanical benefit and may cause undesirable effects such as electrode sticking, metal splashing, or sheet damage.

The challenge is to optimize the welding time because if it is too long causes copper plating of the sheets, splashes of molten metal and excessive indentation and if it is short causes an incomplete fusion and therefore a poor weld.

4.3. Welding Current

To determine the influence of the current intensity on the hardness of the weld point and the strength of the weld sheets, three specimens made with mild steel are tested at the conditions mentioned in table 9.

An increasing current intensity leads to higher hardness values (Fig. 10). Greater heat input accelerates melting and solidification, which can refine the microstructure and enhance local hardness.

Table 9. Experimental welding conditions of the tensile test N°3

Tested specimens	P7	P8	P9
Variable parameter Current intensity [kA]	I=14	I=10	I=12
Input parameters	Mild Steel (DC03), T=18 cycles, e=2 mm and P=6 bars		

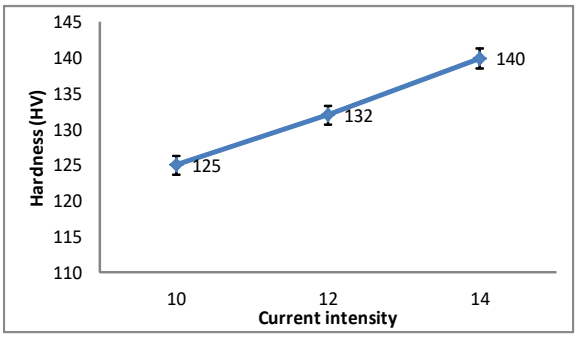

Fig. 10. Effect of welding current

The specimens after the tensile test are shown in figure 11.

Figure 12 shows the evolution curve resulting the load to the displacement until the failure of the spot welded sheets. It is clear that more the current intensity increases, more the breaking load increases.

Fig. 11. Broken specimens after the tensile test for different current intensities: P7 at the top, P8 in the middle and P9 at the bottom

The results (Table 10) show a strong positive correlation between current and weld strength up to 12 kA. The ultimate tensile strength (Rm) increased by over 15% between 10kA and 12kA, but showed minimal gains between 12 and 14 kA, indicating saturation. High current, beyond 14 kA, poses risks such as electrode wear, indentation and weld defects due to overheating. Whereas, if the current intensity is too weak, it will give a weak welding due to the small size of the weld point.

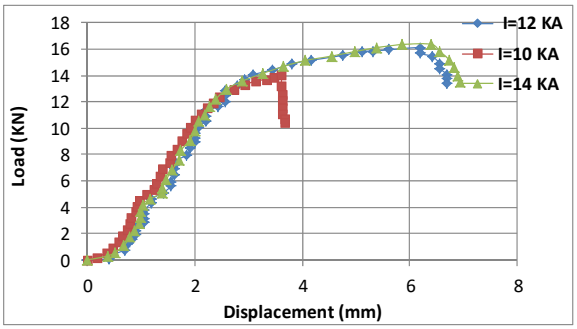

Fig. 12. Effect of the intensity of the current on the mechanical behaviour of the welded sheets according to the test N°3

Table 10. Variation of loads and stresses with current intensity

Results	I= 10 kA	I= 12 kA	I= 14 kA
Fm [kN]	14.031	16.125	16.382
Rm [MPa]	350.781	403.122	409.55

4.4. Thickness

In order to investigate the tensile behaviour of specimens made of mild steel according to the variation of thicknesses, three sheets of 1mm, 1.5mm, and 2mm were tested at conditions mentioned in table 11.

Table 11. Experimental welding conditions of the tensile test N°4

Tested specimens	P10	P11	P12
Variable parameter Sheet thickness [mm]	e=2 mm	e=1.5 mm	e=1 mm
Input parameters	Mild Steel (DC03), T=18 cycles, I=14 KA P=6 bars		

The estimated hardness values on the welding point show that stainless steel 304L presents the highest hardness of 190HV, which is close to that of the base metal. The hardness of galvanized steel Z275 is higher than of mild steel DC03 but both hardness are higher than that of base materials (Fig. 13). In the case of the stainless steel, the negligible variation between the hardness of the base metal and that of the weld point is due to the base microstructure, which is composed primarily of martensite like the fusion zone, which its microstructure consists of martensite and some δ-ferrite due to rapid cooling rates. However, for the two others materials, the hardness upgraded about 20% compared to the base metal. The weld point undergoes very rapid thermal cycles (heating then cooling), which can lead to the formation of harder microstructures.

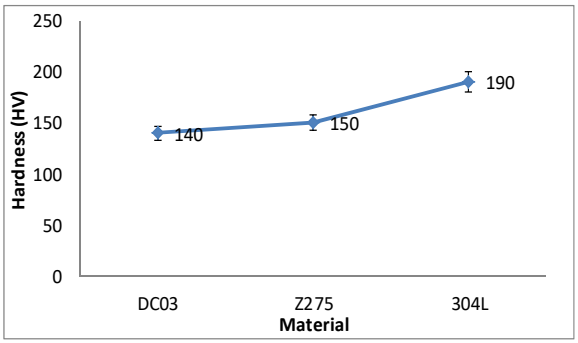

Fig. 13. Effect of material grade

The specimens after the tensile test are shown in figure 14.

Figure 15 represents the evolution curve relating the load to the welded sheets thickness until failure. The analysis of the curves, presented on figure 15, show a flattening at the beginning of the tensile test for the thicknesses of 1mm and of 1.5mm, which is due to the creep of the material at the welding point.

As soon as the thickness increases to 2mm, the material of the welded sheets and that of the welding point behave in the same way.

Consequently, the values of the maximum load and those of the breaking strength are highly distinguished. The increase in the breaking resistance of the assembled sheets is due to the decrease in the heat dissipation speed, favouring a higher resistance of the welding point.

Fig. 14. Broken specimens after the tensile test for different sheet thickness: P10 at the top, P11 in the middle and P12 at the bottom

From table 12, it is clear that when the initial sheet thickness of the welded sheets increases, the breaking strength increases consequently from 1mm to 1.5mm thickness. The Rm value increase significantly for a thickness of 2mm reaching 409,55MPa.

The same remarks are valid for the maximum load Fm, reaching high value of 16.382KN for 2mm thickness.

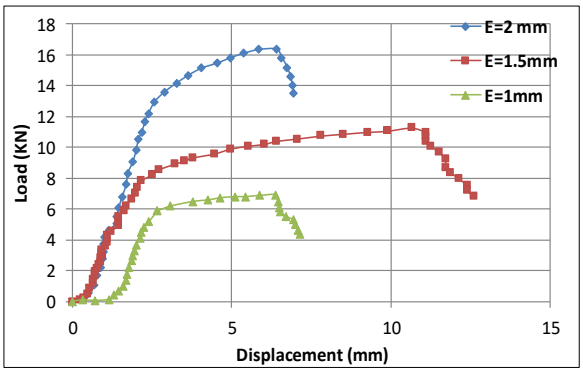

Fig. 15. Effect of initial sheet thickness on the mechanical behaviour of the welded sheets according to the test N°4

Table 12. Variation of loads and stresses as a function of the sheet thickness

Results	e=2 mm	e=1.5 mm	e=1 mm
Fm [kN]	16.382	11.276	6.942
Fe_L [kN]	16.382	9.624	6.318
Fe_H [kN]	16.382	9.734	6.428
Rm [MPa]	409.55	375.88	347.108
Re_L [MPa]	409.55	320.457	315.886
Re_H [MPa]	409.55	324.457	321.396

4.5. Pressure

Applied pressures of 5, 6, and 7 bars were tested on the mild steel following welding conditions listed in table 13. The results indicate that increasing the pressure improves the weld strength up to 7 bars (Rm increased from 382 to 423 MPa). However, beyond 7 bars, mechanical gains plateau, and excessive pressure may lead to defects such as weld crushing, indentation, or metal expulsion.

Optimal pressure ensures proper nugget formation and mechanical locking, whereas too low or too high pressure can compromise weld quality. The specimens after the tensile test are shown in figure 16.

Figure 17 shows the evolution curve relating the load to the displacement for different pressures applied between the electrodes until failure. It can be seen that the evolution of the tensile force as a function of the displacement is practically identical for the different pressures until the failure begins to occur where a small shift is observed.

Table 13. Experimental welding conditions of the tensile test N°5

Tested specimens	P13	P14	P15
Variable parameter Pressure level (bars)	P=6	P=7	P=5
Input parameters	Mild steel (DC03), T=18 cycles, I=14 KA and e=2 mm		

Fig. 16. Broken specimens after the tensile test for different applied pressures: P13 at the top, P14 in the middle and P15 at the bottom

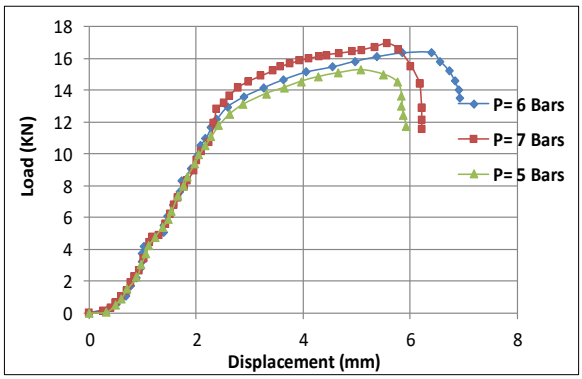

Fig. 17. Effect of the welding pressure on the mechanical behavior welded sheets according to the test N°5

In terms of values presented in table 14, there is a slight variation with regard to the tensile force but a significant variation in terms of the breaking load, which increases with the increase in the pressure between electrodes.

Table 14. Variation of loads and stresses as a function of the pressure level

Results	P=5 bars	P=6 bars	P=7 bars
Fm [kN]	15.28	16.382	16.924
Rm [MPa]	382.002	409.55	423.122

The results indicate that increasing the pressure improves the weld strength up to 7bars (Rm increased from 382.002 to 423.112MPa) where proper nugget formation is observed. Whereas too low or too high pressure can compromise weld quality, especially, excessive pressure may lead to defects such as weld crushing, indentation or metal expulsion. On the other hand, an insufficient pressure causes an increase in breaking resistance, splashes of molten metal or burnt spots and abnormal wear of the electrodes.

By analysing these results, it can be said that the influence of the pressure between electrodes is not very significant with regard to the mechanical behaviour of

the welded structures but it tends to improve the breaking resistance by increasing the diameters of the welded points under the increasing of the pressure effect.

5. CONCLUSIONS

This study provided a comprehensive experimental evaluation of the influence of resistance spot welding parameters on the mechanical performance of weld sheet structures. It offers original insights into the optimization of process parameters, namely electrode pressure, current intensity, and welding time to enhance weld quality and structural reliability. The results highlight that material type and sheet thickness have a significant effect on the weld strength. Stainless steel showed the highest performance with a maximum tensile load and breaking strength, compared to those for galvanized and mild steels. The high performance of stainless steel is attributed to its initial microstructure formed with martensite, which is favorable to higher mechanical properties of the weld point, while the relatively lower strength of others studied steels may be due to the incomplete transformation of the initial microstructure to martensite. The presented results confirm that the mechanical performance of resistance spot welded joints depends on both the intrinsic properties of the materials and the process conditions. The optimal configuration lies in a balanced combination of material choice and process control, avoiding extremes that would cause premature wear or joint weakening.

As a perspective, future work will address the influence of electrode life and wear on joint quality and machine maintenance, in order to develop a more robust and predictive spot welding process.

REFERENCES

[1] **Chen L., Zhang Y., Xue X., Wang B., Yang J., Zhang Z., Tyrer N., Barber G.C.,** *Investigation on shearing strength of resistance spot-welded joints of dissimilar steel plates with varying welding current and time*. Journal of Materials Research and Technology, vol. 16, 2022, pp. 1021-1028.

[2] **Shojaee M., Tolton C., Midawi A. R. H., Butcher C., Ghasemi-Armaki H., Worswick M., Biro E.,** *Influence of loading orientation on mechanical properties of spot welds*, International Journal of Mechanical Sciences, vol. 224, 2022, 107327.

[3] **Chen G., Xue W., Jia Y., Shen S., Liu G.,** *Microstructure and mechanical property of WC-10Co/RM80 steel dissimilar resistance spot welding joint*. Materials Science & Engineering A, vol. 776, 2020, 139008.

[4] **Mousavi-Anijdan S.H., Sabzi M., Ghobeiti-Hasab M., Roshan-Ghiyas A.,** *Optimization of spot welding process parameters in dissimilar joint of dual phase steel DP600 and AISI 304 stainless steel to achieve the highest level of shear-tensile strength*. Materials Science & Engineering A, vol. 726, 2018, pp. 120-125.

[5] **Shirmohammadi D., Movahedi M., Pouranvari M.,** *Resistance spot welding of martensitic stainless steel: Effect of initial base metal microstructure on weld microstructure and mechanical performance*, Materials Science & Engineering A, vol. 703, 2017, pp. 154-161.

[6] **Costa H. R. M., Reis J. M. L., Souza J. P. B., Pacheco P. M. C. L., Aguiar R. A. A., Barros S. D.,** *Experimental investigation of the mechanical behaviour of spot welding–adhesives joints*, Composite Structures, vol. 133, 2015, pp. 847-852.

[7] **Eshraghi M., Tschopp M. A., Zaeem M. A., Felicelli S. D.,** *Effect of resistance spot welding parameters on weld pool properties in a DP600 dual-phase steel: A parametric study using thermo-mechanically coupled finite element analysis*, Materials and Design, vol. 56, 2014, pp. 387-397.

[8] **Florea R. S., Bammann D. J., Yeldell A., Solanki K. N., Hammi Y.,** *Welding parameters influence on fatigue life and microstructure in resistance spot welding of 6061-T6 aluminum alloy*, Materials and Design, vol. 45, 2013, pp. 456-465.

[9] **Lin H. J., Chang H. S.,** *In-process monitoring of micro series spot welding using dual accelerometer system*, Welding in the World, vol. 63, no. 6, 2019, pp. 1641-1654.

[10] **Wang X., Zhang V.,** *Effects of welding procedures on resistance projection welding of nuts to sheets*, ISIJ International, vol. 57, no. 12, 2017, pp. 2194-2200.

[11] **Han G., Ha S., Marimuthu K.P., Murugan S.P., Park Y., Lee H.,** *Shape optimization of square weld nut in projection welding*, The International Journal of Advanced Manufacturing Technology, vol. 113, 2021, pp. 1915-1928.

[12] **François D.,** *Essais de rupture*, Techniques de l'ingénieur M126-3, 1996.

[13] *Stainless Steel 304* L1.4307, Material Data Sheet (11/2017), Thyssenkrupp Materials (UK) Ltd., https://www.thyssenkrupp-materials.co.uk/stainless-steel-304l-14307.html

[14] *Feuillard laminé à froid, Aciers inoxydables* (6/2017), ars METAL, France, http://www.ars-metal.com/uploads/produits/a29feb5bde3c133d826ca8c372ba23fc.pdf

[15] *DC03 Steel Properties* (12/2020), GNEE Multinational Trade Co. (China) Ltd., https://www.gneeppgi.com/info/dc03-steel-properties-52613444.html